Genome-wide analysis of gene expression profile in the respiratory tree of sea cucumber (*Apostichopus japonicus*) in response to hypoxia conditions

LIBIN ZHANG[1,2], QIMING FENG[1,2,3], KUI DING[1,2,3], LINA SUN[1,2], DA HUO[1,2,3], YAN FANG[4], TAO ZHANG[1,2] AND HONGSHENG YANG[1,2]

[1]CAS Key Laboratory of Marine Ecology and Environmental Sciences, Institute of Oceanology, Chinese Academy of Sciences, 7 Nanhai Road, Qingdao 266071, China, [2]Laboratory for Marine Ecology and Environmental Science, Qingdao National Laboratory for Marine Science and Technology, Qingdao 266071, China, [3]University of Chinese Academy of Sciences, 19A Yuquan Rd, Shijingshan District, Beijing 100049, China, [4]School of Agriculture, Ludong University, 186 Hongqizhong Road, Yantai 264025, China

The sea cucumber Apostichopus japonicus *is a deposit-feeder and vital for marine benthic ecosystems. Hypoxia can influence the behaviour and even lead to massive mortality in* A. japonicus *in the wild. It is important to understand the molecular responses of* A. japonicus *when exposed to acute changes in dissolved oxygen (DO) concentration. In this study, RNA-seq provided a general overview of the gene expression profiles of the respiratory tree of* A. japonicus *exposed to DO of 8 mg l^{-1} (DO8), 4 mg l^{-1} (DO4) and 2 mg l^{-1} (DO2) conditions. Differentially expressed genes (DEGs) screening with the NOISeq method identified 51, 59 and 61 DEGs according to the criteria of fold change ≥2 and divergence probability ≥0.8 in the comparisons of DO2 vs DO4, DO2 vs DO8 and DO4 vs DO8, respectively. Gene ontology analysis showed that 'cellular process' and 'binding' had the most enriched DEGs in the categories of 'biological process' and 'molecular function', respectively (catalytic activity also had the most enriched DEGs in the category of 'molecular function' based on the comparison of DO2 vs DO8), while 'cell' and 'cell part' had the most enriched DEGs in the category of 'cellular component'. The DEGs were mapped to 79, 81 and 104 pathways in the KEGG database, and 8, 29 and 16 pathways were significantly enriched, respectively. The DO-specific DEGs identified in this study of the respiratory tree are important targets for further research into the biochemical mechanisms involved in the response of the sea cucumber to changes in the DO concentration.*

INTRODUCTION

Dissolved oxygen (DO) is a critical constraint that can affect aquatic animals in ecological systems. If the DO level falls to hypoxic concentrations, the habitability decreases rapidly for aerobic organisms (Deutsch *et al.*, 2011). DO concentrations below ~60 μM (1.92 mg l^{-1}), known as hypoxia, are lethal for more than 50% of marine benthic animals, and this proportion increases to more than 90% when the DO concentration falls below ~10 μM (0.32 mg l^{-1}) (Vaquer-Sunyer & Duarte, 2008). Hypoxia has become a severe problem and it can have significant deleterious effects on ecological dynamics and fishery sustainability throughout coastal ecosystems worldwide (Nestlerode & Diaz, 1998; Diaz, 2001).

The sea cucumber *Apostichopus japonicus* is a deposit-feeder and vital for marine benthic ecosystems, and it is a common temperate species that lives in the shallow sea off

north-west China (Liao, 1980; Sloan, 1984). Due to its high nutritional value and health benefits, *A. japonicus* is highly desirable in the East Asian consumer market, particularly in China (Zhou *et al.*, 2014; Ren *et al.*, 2017). *Apostichopus japonicus* is now the most common economic species that is released and cultured in the marine ranches of northern China (Zhang *et al.*, 2015*b*). O$_2$ is a primary factor that affects sea cucumbers living on the sea floor. When the DO concentration dropped to a hypoxic extent in some parts of Laizhou Bay during 2013, *A. japonicus* climbed to the tops of artificial or natural reefs, where individuals attached and overlapped with each other. If hypoxia lasts for several days, massive mortality of *A. japonicus* might occur.

As is shown in the previous studies, asteroids such as *Asterias rubens* (Theede *et al.*, 1969), *Asterias rubens* (Holm *et al.*, 2008; Oweson *et al.*, 2010) and *Ctenodiscus crispatus* (Shick, 1976) are sensitive to hypoxia. Hypoxia also has negative effects on the regeneration and reproduction of brittle star, *Amphiura filiformis* (Nilsson & Sköld, 1996). The green sea urchin, *Strongylocentrotus droebachiensis*, also shows low tolerance to hypoxia with low gonad growth and total food consumption (Siikavuopio *et al.*, 2007). Previous studies

Corresponding author:
H. Yang
Email: hshyang@qdio.ac.cn

2039

have tried to understand the biological basis and mechanism of movement and feeding behaviours (Pan *et al.*, 2015; Sun *et al.*, 2015; Zhang *et al.*, 2015*a*), growth (Li & Li, 2010), development (Kashenko, 2000), respiration and excretion (Sui *et al.*, 2010), the energy budget (Yuan *et al.*, 2010), immune responses (Wang *et al.*, 2008, 2011), physiological responses in terms of osmoregulation and heat shock protein expression (Dong *et al.*, 2008; Meng *et al.*, 2011), molecular responses to pathogen challenge (Shao *et al.*, 2013; Zhang *et al.*, 2013, 2014) and the molecular responses of differentially expressed genes (DEGs) in the aestivation stage (Zhao *et al.*, 2014) and intestine regeneration stage (Sun *et al.*, 2013) in *A. japonicus*. In these studies, the effects of environmental factors were investigated, such as temperature, salinity, light, pH and water flow. However, few studies have considered the effects of hypoxia on the behaviour, physiology and molecular responses of DEGs in *A. japonicus*. Thus, the molecular mechanisms responsible for adaptation to acute changes in the DO concentration are poorly understood.

In recent years, global change and human activities have intensified, and anthropogenic nutrient loading has increased the frequency and severity of hypoxia in estuaries and semi-enclosed seas (Grantham *et al.*, 2004). Hypoxia poses a great challenge to the aquaculture of *A. japonicus*. The respiratory tree, which is the respiratory organ in *A. japonicus*, might be sensitive to the stress induced by a low DO concentration and the differential expression of genes may occur in different DO environments. Thus, the aim of this study was to obtain a better understanding of the molecular responses of *A. japonicus* when exposed to changes in the ambient acute DO concentration in order to provide a theoretical basis for hypoxia risk prevention and control in aquaculture.

MATERIALS AND METHODS

Animals

The sea cucumbers, *A. japonicus* involved in this study were not endangered or protected. In total, 60 fresh and healthy sea cucumbers, *A. japonicus* were collected from the coast of Laizhou, China, with wet weights of 80–130 g. After weighing, they were acclimated in tanks containing aerated sand-filtered seawater (salinity 30‰, pH 8.0) at $15 \pm 0.5\,^{\circ}C$ for one week before use and they were fed once each day at 8:00 am during this period. All of the animals were then assigned randomly to three groups (20 individuals in each group). One group of sea cucumbers was maintained as the control group with high DO water (DO8) at around $8\ \mathrm{mg\ l^{-1}}$, whereas the other two groups were kept in seawater with nitrogen injection where the DO concentration gradually decreased to $\sim 4\ \mathrm{mg\ l^{-1}}$ DO (DO4) and $2\ \mathrm{mg\ l^{-1}}$ DO (DO2) in 1 h, which is defined as hypoxia (Diaz & Rosenberg, 1995), and they were maintained for three days. Next, nine individuals were selected randomly from each group (three groups) and dissected rapidly, where the respiratory tree was sampled and preserved in liquid nitrogen for RNA extraction and sequencing.

RNA isolation and sequencing

According to the manufacturer's instruction, an RNeasy mini kit (Qiagen Inc., Hilden, Germany/Cat No. 74104) including

DNase treatment was used to isolate total RNA from nine samples of the respiratory tree from each group (DO2, DO4 and DO8). The RNA samples from every three individuals in the same group were pooled in equal amounts for library construction as one replicate (three replicates in each group). Libraries were prepared from the nine RNA pools by Beijing Genomics Institute, Shenzhen, China (BGI-Shenzhen). Strict quality control (QC) was applied in each experimental step to obtain highly reliable sequencing data. Magnetic beads with poly-T-oligos attached were used to isolate poly(A) mRNA. The target RNA was then purified. The target RNA was fragmented into short sequences, reverse-transcribed into single-strand cDNA using the N6 random primer (Promega, Madison, WI, USA), and synthesized into double-stranded cDNA (dscDNA) with DNA polymerase I and RNase H (Promega, Madison, WI, USA). Next, the end of the dscDNA was repaired and ligated with a sequencing adapter. The ligation product was amplified using specific primers. The PCR product was denatured by heating and the single strand DNA was cyclized using splint oligo and DNA ligase. Finally, high throughput sequencing was performed with the prepared cDNA libraries using the BGISEQ-500 RS platform at BGI-Shenzhen.

Data filtering, read mapping and sequence QC

QC was applied to the raw reads from primary sequencing to determine whether a resequencing step was required. Data filtering was performed after QC to decrease the data noise. Reads with adapters, reads with more than 10% unknown bases, and low quality reads (if the percentage of low quality bases was over 50% in a read, a low quality base was a base with a sequencing quality of no more than 5%) were removed. After filtering, the remaining reads were designated as 'clean reads'. Clean reads were mapped to the reference transcriptome in a 454 sequence transcriptomic database for *A. japonicus* (NCBI accession nos. SRA020994 and SRA046386) (Sun *et al.*, 2011; Du *et al.*, 2012) using Bowtie2 (Langmead *et al.*, 2009) and to the reference genome using hierarchical indexing for spliced alignment of transcripts (HISAT) (Kim *et al.*, 2015). The alignment was also subjected to QC to determine whether resequencing was necessary. The distribution of the reads in the reference genes and the mapping ratio were calculated using the alignment data. If the alignment result passed QC, deep analysis was implemented, including gene expression and related analyses based on gene expression.

Gene quantification, DEG screening and functional classification

Transcripts that were isoforms of the same gene were determined by computing maximum likelihood abundance estimates with the quantification tool for RNA-Seq by Expectation Maximization (RSEM) (Li & Dewey, 2011).

The fragments per kilobase of exon per million fragments mapped (FPKM) method (Mortazavi *et al.*, 2008) was used to calculated gene expression levels. The NOISeq method (Tarazona *et al.*, 2011) was used to identify the DEGs in groups of sea cucumbers exposed to different DO concentrations. In the NOISeq method, the gene expression level in each group was used to compute $\log_2$ ratio (fold change), M, and

the absolute difference value, D, for all paired conditions in order to build a noise distribution model. For a specific gene, the P-value estimated how much M and D both diverged from the noise distribution. The criteria of fold change ≥2 and divergence probability ≥0.8 were used as thresholds to screen the DEGs.

To identify the functional classifications of DEGs, Gene Ontology (GO) terms were determined for the DEGs using Blast2GO (Hemandez et al., 2006) and pathway analysis was performed based on the Kyoto Encyclopedia of Genes and Genomes (KEGG) database. The gene numbers were computed for every term and the DEGs were subjected to a hypergeometric test, where significantly enriched GO terms were determined based on a P-value ≤ 0.05 after Bonferroni correction (Abdi, 2007). The formula used to calculate the P-values for determining significantly enriched KEGG pathways was the same as that used for GO analysis. In addition, the significantly enriched KEGG pathways were determined based on corrected P-values ≤ 0.05. A strict algorithm based on Bonferroni correction (Abdi, 2007) was employed to calculate the P-values.

Real-time PCR (RT-qPCR) validation

RT-qPCR was performed in order to validate the RNA-seq results obtained for some significant DEGs. Primers (Table 1) were designed for optimal performance with primer3 according to the sequence information in the transcriptome database. The input RNA used for template cDNA synthesis was run in triplicate of each group. According to our previous study (Sun et al., 2013), the first strand cDNA was synthesized in a 25-µl reaction system. Eppendorf Mastercycler® eprealplex (Eppendorf, Hamburg, Germany) was used to determine the mRNA expression levels with the SYBR Green® real-time PCR assay. The total volume used for amplification was 20 µl, which comprised 8 µl of RNase-free water, 10 µl of SYBR GreenMasterMix (Takara), 1 µl of diluted cDNA and 0.5 µl each of the

forward and reverse primers (10 mM). Thermal cycling was performed according to the following procedure: 95°C for 5 s, followed by 40 cycles at 95°C for 10 s, 60°C for 20 s and 72°C for 30 s. The specificity of the amplification products was validated by melting curve analysis. All of the data were expressed as the mean ± SD and the threshold for significant differences was $P < 0.05$. Significant differences between groups for each gene were determined by one-way ANOVA with Tukey's test using SPSS 18 software (IBM Corp., Armonk, NY, USA).

RESULTS

Analysis of the sequencing data quality

Libraries of nine samples from three different groups (DO2, DO4 and DO8) were constructed from sea cucumber respiratory tree samples using RNA-Seq. In total, there were 24,097,736 raw sequencing reads and 23,847,854 clean reads were obtained after filtering out low quality sequences. The clean reads from the three groups were submitted to NCBI (accession no. GSE100042). The sequencing raw reads number and clean reads number for each sample were listed in Table 2. Among these reads, the statistics for read alignments with reference genes and the whole genome, i.e. the total mapped reads rate and unique match rate were shown in Table 3.

Strict QC was applied to each sample (Table S1) to evaluate the quality of the sequencing data. Saturation analysis based on the sequencing data indicated that when a certain amount of sequencing reads were reached, the growth curve flattened for the identified genes and the number of genes identified tended to reach saturation (Figure S1). The sequencing randomness assessment determined the distribution of the reads and the aligned reads appeared to be distributed evenly in the three libraries (Figure S2).

Table 1. Selected genes and primers designed for real-time PCR.

Gene name	Primer sequence
Lysozyme	5′-ATCGGTTGACGAGTAGAGGTA-3′5′-ATAGTCGCTGCTGTGGAAG-3′
Chloride channel calcium activated 3-like	5′-GCAGAAGGAGGGTTGTATT-3′5′-TAGTAGCATTTGCCGAAGT-3′
Phytanoyl-CoA dioxygenase	5′-TCTGAGGAAGCATAGTGGC-3′5′-CTGGGAGATGGGAGTGAAT-3′
Counting factor associated protein D-like (CAFD)	5′-ACTGGACGGGAACTATTGG-3′5′-GAACTTGACGAACCCTTTG-3′
Major vault protein (MVP)	5′-CTGGACCAAAGACAAC-3′5′-GAATCAAGACGAGGAG-3′

Table 2. Summary of the sequencing data obtained for each sample.

Sample	Sequencing strategy	Raw data size (bp)	Raw reads number	Clean data size (bp)	Clean reads number	Clean data rate (%)
DO2-1	SE50	1,206,859,500	24,137,190	1,203,241,600	24,064,832	99.70
DO2-2	SE50	1,206,865,900	24,137,318	1,204,075,500	24,081,510	99.76
DO2-3	SE50	1,206,867,750	24,137,355	1,198,667,550	23,973,351	99.32
DO4-1	SE50	1,197,923,250	23,958,465	1,141,700,600	22,834,012	95.30
DO4-2	SE50	1,198,006,600	23,960,132	1,190,375,750	23,807,515	99.36
DO4-3	SE50	1,206,871,850	24,137,437	1,202,445,000	24,048,900	99.63
DO8-1	SE50	1,206,863,200	24,137,264	1,202,985,650	24,059,713	99.67
DO8-2	SE50	1,206,861,250	24,137,225	1,188,561,300	23,771,226	98.48
DO8-3	SE50	1,206,862,000	24,137,240	1,199,481,450	23,989,629	99.38

Table 3. Statistics for read alignments with reference genes and the whole genome.

Mapping reference	Sample	Total reads	Total mapped reads (%)	Unique match (%)	Multi-position match (%)	Total unmapped reads (%)
Reference genes	DO2-1	24,064,832	20.59	14.38	6.21	79.41
	DO2-2	24,081,510	16.56	11.42	5.14	83.44
	DO2-3	23,973,351	33.17	23.69	9.48	66.83
	DO4-1	22,834,012	13.07	9.19	3.88	86.93
	DO4-2	23,807,515	20.87	15.00	5.87	79.13
	DO4-3	24,048,900	24.37	17.19	7.18	75.63
	DO8-1	24,059,713	25.05	17.33	7.72	74.95
	DO8-2	23,771,226	21.73	15.21	6.52	78.27
	DO8-3	23,989,629	17.89	12.41	5.48	82.11
Genome	DO2-1	24,064,832	70.97	41.02	29.95	29.04
	DO2-2	24,081,510	70.44	40.87	29.57	29.55
	DO2-3	23,973,351	72.13	41.45	30.68	27.87
	DO4-1	22,834,012	60.60	33.51	27.09	39.40
	DO4-2	23,807,515	67.24	37.31	29.93	32.76
	DO4-3	24,048,900	73.89	43.05	30.84	26.11
	DO8-1	24,059,713	73.00	41.52	31.48	27.00
	DO8-2	23,771,226	74.22	42.43	31.79	25.78
	DO8-3	23,989,629	63.30	36.31	26.99	36.70

DEG analysis

RNA-seq provided a general overview of the gene expression profiles in the respiratory trees of *A. japonicus* specimens exposed to different DO concentrations of 2, 4 and 8 mg l^{-1}. In total, 27,214 unigenes were identified in the three different groups. The three samples from the same DO environments were grouped into DO2, DO4 and DO8. DEG screening with the NOISeq method identified 51, 59 and 61 DEGs according to the criteria of fold change ≥ 2 and divergence probability ≥ 0.8 in the comparisons of DO2 *vs* DO4, DO2 *vs* DO8 and DO4 *vs* DO8, respectively (Figure 1).

In particular, 30 downregulated DEGs (0.11%, 30/27,214) and 21 upregulated DEGs (0.08%, 21/27,214) were identified based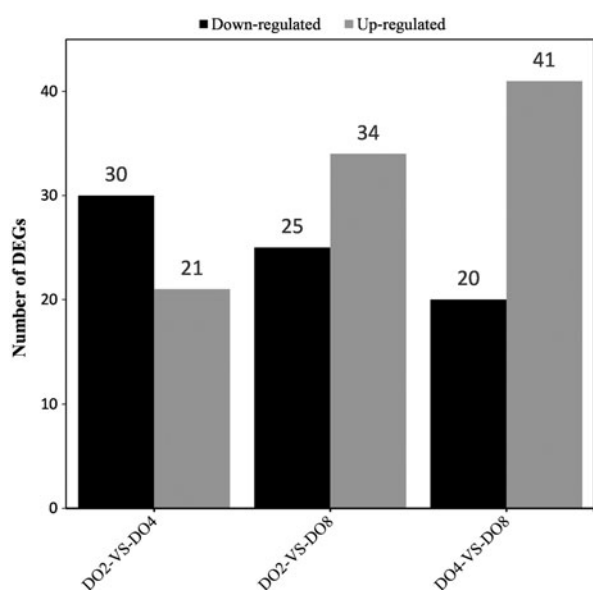 on the comparison of DO2 *vs* DO4, 25 downregulated DEGs (0.09%, 25/27,214) and 34 upregulated DEGs (0.12%, 34/27,214) were identified based on the comparison of DO2 and DO8, and 20 downregulated DEGs (0.07%, 20/27,214) and 46 upregulated DEGs (0.15%, 41/27,214) were identified based on the comparison of DO4 *vs* DO8.

The down- or upregulated DEGs annotated based on these three comparisons are listed in Tables S2–S4. Several DO-specific expression genes were found. DEGs such as *ATP synthase subunit f, mitochondrial, cyclophilin A isoform 1, phytanoyl-CoA dioxygenase, peroxisomal-like* and *thioredoxin* had significantly higher expression levels in the DO2 and DO4 groups compared with the DO8 group, where the mean expression level was 0.01. In addition, other genes such as *cysteine-rich secretory protein LCCL domain containing 2-like, major vault protein* and *RNA-directed DNA polymerase from mobile element jockey-like* had significantly higher expression levels in the DO2 group compared with the DO4 and DO8 groups, with a mean expression level of 0.01. Moreover, *counting factor associated protein D-like* and *scavenger receptor cysteine-rich protein precursor* had significantly higher expression levels in the DO8 group compared with the DO2 and DO4 groups, where the mean expression level was 0.01.

Based on the primary results, some genes appeared to have functions that were important for understanding the response of the respiratory tree in *A. japonicus* to different DO concentrations, as shown in Table 4. The key DEGs associated with different DO concentrations were classified into four groups.

GO classification

Complete functional information can be obtained by assigning DEGs to three major categories ('cellular component', 'molecular function' and 'biological process'). In order to identify the functions of the DEGs, they were subjected to GO analysis. GO term enrichment analysis detected 17, 2 and 26 significantly over-represented enriched GO terms based on the comparisons of DO2 *vs* DO4, DO2 *vs* DO8 and DO4 *vs* DO8, respectively, where $P < 0.05$.

Fig. 1. Statistics for the DEGs. The *x*-axis represents the pairwise comparisons and the *y*-axis shows the number of DEGs screened. Black bars denote downregulated genes and grey bars are upregulated genes.

Table 4. Key DEGs associated with the effects of different DO concentrations.

Gene	Gene ID	Means-DO2	Means-DO4	Means-DO8
Key DEGs associated with stimuli response and signal transduction				
Calcium-activated chloride channel regulator 1-like	scaffold778.29	0.21	29.22	18.12
Chloride channel calcium activated 3-like	scaffold778.27	5.46	118.21	245.16
Clarin-1-like	scaffold787.13	7.25	0.073	15.95
CUB and zona pellucida-like domain-containing protein 1-like, partial	scaffold209.31	0.01	46.50	0.01
Cubilin	scaffold946.7	0.48	0.01	12.33
Fucose mutarotase	scaffold2777.1	7.16	11.43	0.01
Gamma-aminobutyric acid type B receptor subunit 1-like	scaffold510.15	0.01	7.85	10.43
Ileal sodium/bile acid cotransporter-like	scaffold942.9	2.32	4.25	91.51
Pituitary tumour-transforming gene 1 protein-interacting protein-like isoform 1	scaffold2488.6	13.77	0.01	25.02
Transmembrane protease, serine 3-like, partial	scaffold463.27	13.25	0.01	0.06
Key DEGs associated with metabolism				
60S ribosomal protein L35-like	scaffold2928.2	56.52	0.57	324.11
60S ribosomal protein L35-like	scaffold3023.2	56.52	0.57	324.11
60S ribosomal protein L35-like	scaffold3030.2	56.52	0.57	324.11
60S ribosomal protein L35-like	scaffold3089.2	56.52	0.57	324.11
Alcohol dehydrogenase [NADP+]-like	scaffold207.26	0.01	1.74	11.48
ATP synthase subunit f, mitochondrial	scaffold1341.9	37.66	147.48	0.01
Cell division cycle 2	scaffold532.9	0.01	35.27	1.24
Counting factor associated protein D-like	scaffold2429.3	0.01	0.01	14.94
Epidermal retinol dehydrogenase 2-like	scaffold305.2	93.97	1.77	6.01
Extracellular serine proteinase-like	scaffold769.20	0.09	0.01	17.28
Phytanoyl-CoA dioxygenase, peroxisomal-like	scaffold118.42	15.30	57.83	0.01
Polyprotein	scaffold3.4	0.72	0.01	13.00
Retrovirus polyprotein, putative-like	scaffold200.5	0.01	0.02	13.66
Reverse transcriptase	scaffold1946.6	0.01	41.54	2.14
Reverse transcriptase-like protein-like	add.scaffold1043.4	0.52	2.08	54.09
RNA-directed DNA polymerase from mobile element jockey-like	add.scaffold560.16	0.01	1.42	28.28
RNA-directed DNA polymerase from mobile element jockey-like	scaffold559.15	9.92	0.01	0.01
RNA-directed DNA polymerase from mobile element jockey-like	scaffold657.18	6.34	217.42	11.38
RNA-directed DNA polymerase from mobile element jockey-like	scaffold716.20	0.32	164.89	2.43
Spermidine synthase-like	scaffold1647.2	0.01	17.61	2.05
Threonyl-tRNA synthetase, cytoplasmic, putative	scaffold2224.1	13.37	0.01	6.61
Carboxypeptidase A2-like	scaffold3179.1	4.94	15.73	0.01
Key DEGs associated with immune defence				
Cyclophilin A isoform 1	scaffold245.2	16.66	37.46	0.01
Fibrinogen C domain-containing protein 1-B, partial	scaffold561.13	1.75	0.01	26.75
Fibrinogen-like protein 1-like	add.scaffold1306.4	0.96	7.00	55.67
Fibrinogen-like protein 1-like	scaffold907.21	185.69	17.34	7.25
Fibrinogen-like protein A	scaffold352.13	7.01	0.61	56.14
Fibrinogen-like protein A	scaffold955.14	79.93	1.14	1.48
Fibrinogen-like protein A	scaffold955.15	66.26	1.65	1.08
Ficolin (collagen/fibrinogen domain containing) 1 precursor	scaffold1149.6	6.02	36.51	173.59
IgGFc-binding protein, partial	scaffold114.44	0.10	23.94	19.73
Lysozyme	scaffold469.3	3.04	122.43	145.41
Major vault protein	scaffold2850.1	25.39	0.01	0.01
Protein NLRC3-like	scaffold169.52	0.55	0.01	10.49
Protein NLRC3-like, partial	scaffold169.42	9.02	0.49	112.96
Key DEGs associated with hypoxia and apoptosis				
Glutaredoxin-related protein 5	scaffold327.41	8.45	0.04	22.13
Thioredoxin	scaffold2817.2	85.70	151.71	0.01
Angiopoietin-related protein 4-like	scaffold1306.4	96.12	2.45	0.47
Scavenger receptor cysteine-rich protein precursor	scaffold163.8	0.01	0.01	10.29
THO complex subunit 1	scaffold2243.2	12.99	1.24	122.51

In the three comparisons, 'cellular process' and 'binding' had the most enriched DEGs in the categories of 'biological process' and 'molecular function', respectively (catalytic activity also had the most enriched DEGs in the category of 'molecular function' based on the comparison of DO2 *vs* DO8), while 'cell' and 'cell part' had the most enriched DEGs in the category of 'cellular component' (Figure 2).

KEGG classifications

Genes usually interact with each other and play roles in specific biological functions. The DEGs were also mapped to KEGG metabolic and regulatory pathways with a correct P-value cutoff of < 0.05. The DEGs detected in the comparisons of DO2 *vs* DO4, DO2 *vs* DO8 and DO4 *vs* DO8 affected
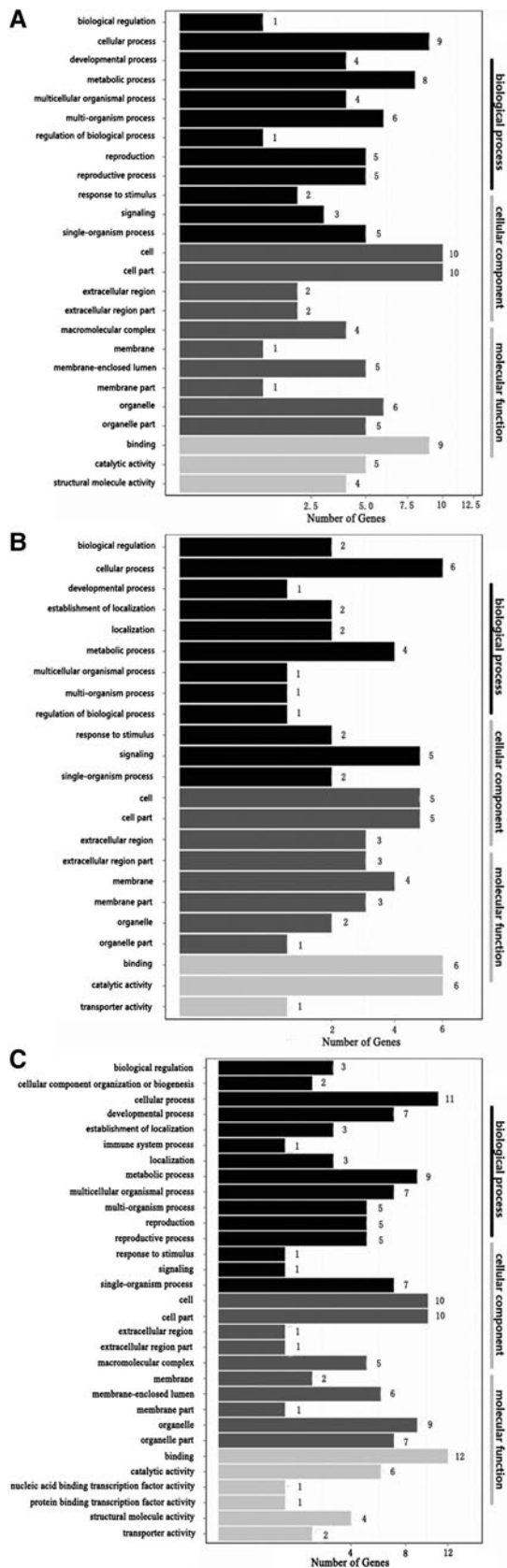
Fig. 2. GO functional classifications of DEGs based on each pairwise comparison. The *x*-axis shows the number of DEGs (as the square root of the value). The *y*-axis shows the GO terms. All of the GO terms are grouped into three ontologies: blue = biological process, brown = cellular component and orange = molecular function (A. DO2 *vs* DO4, B. DO2 *vs* DO8, C. DO4 *vs* DO8).

a range of KEGG pathways. The top 20 KEGG enrichment results are shown in Figure 3. The DEGs were mapped to 79, 81 and 104 pathways in the KEGG database, and 8, 29 and 16 pathways were significantly enriched, respectively (corrected *P*-value <0.05). The most representative KEGG pathways included Ribosome (ko03010), MicroRNAs in cancer (ko05206), and Hematopoietic cell lineage (ko04640) in the comparison of DO2 *vs* DO4; Epstein-Barr virus infection (ko05169), Viral myocarditis (ko05416) and Pertussis (ko05133) in the comparison of DO2 *vs* DO8; and HIF-1 signalling pathway (ko04066), Ribosome (ko03010), and Carbon metabolism (ko01200) in the comparison of DO4 *vs* DO8.

Validation of DEG analyses

In order to validate the DEGs identified, five genes (chloride channel calcium activated 3-like, phytanoyl-CoA dioxygenase, counting factor associated protein D-like, major vault protein and lysozyme) were selected to determine their relative mRNA expression levels using RT-qPCR. The results showed that the expression levels obtained for these five genes using RT-qPCR were similar to the DEG analysis patterns (Figure 4) under different DO exposure levels. This comparison of the data obtained by DEG analysis and the data produced using RT-qPCR suggest that the sequencing data were credible.

DISCUSSION

Oxygen (O_2) is a very important constraint on marine ecosystems. Many biological and physiological processes are related to O_2 thresholds, which restrict the activity and habitat of marine organisms (Deutsch *et al.*, 2011). *Apostichopus japonicus* is very sensitive to changes in the DO concentration and its optimal DO range is $4-8 \, \mathrm{mg} \, \mathrm{l}^{-1}$. However, in some ocean areas, the DO concentration in the water may drop to $2 \, \mathrm{mg} \, \mathrm{l}^{-1}$ or even lower during the hot season. When *A. japonicus* is exposed to low DO concentrations, physiological stress may occur and various molecular regulation mechanisms can be affected. The results showed that the exposure of *A. japonicus* to different DO concentrations was associated with thousands of transcriptional variations. Numerous stimuli response, immune defence and signal transduction related genes differed in terms of their expression levels when *A. japonicus* was exposed to different DO concentrations. These genes may be excellent candidates for further studies of the molecular mechanisms associated with behaviour and physiology in *A. japonicus* under different DO concentrations.

Genes associated with stimuli response and signal transduction

If the DO concentration in seawater is excessively low, this can serve as a stimulus for *A. japonicus*, where several key genes are associated with responses to stimuli and signal transduction processes.

Calcium-activated chloride channels are involved in various physiological processes, such as oocyte fertilization, transepithelial transport and the excitability of neurons and muscle cells (Eggermont, 2004). Calcium-activated chloride
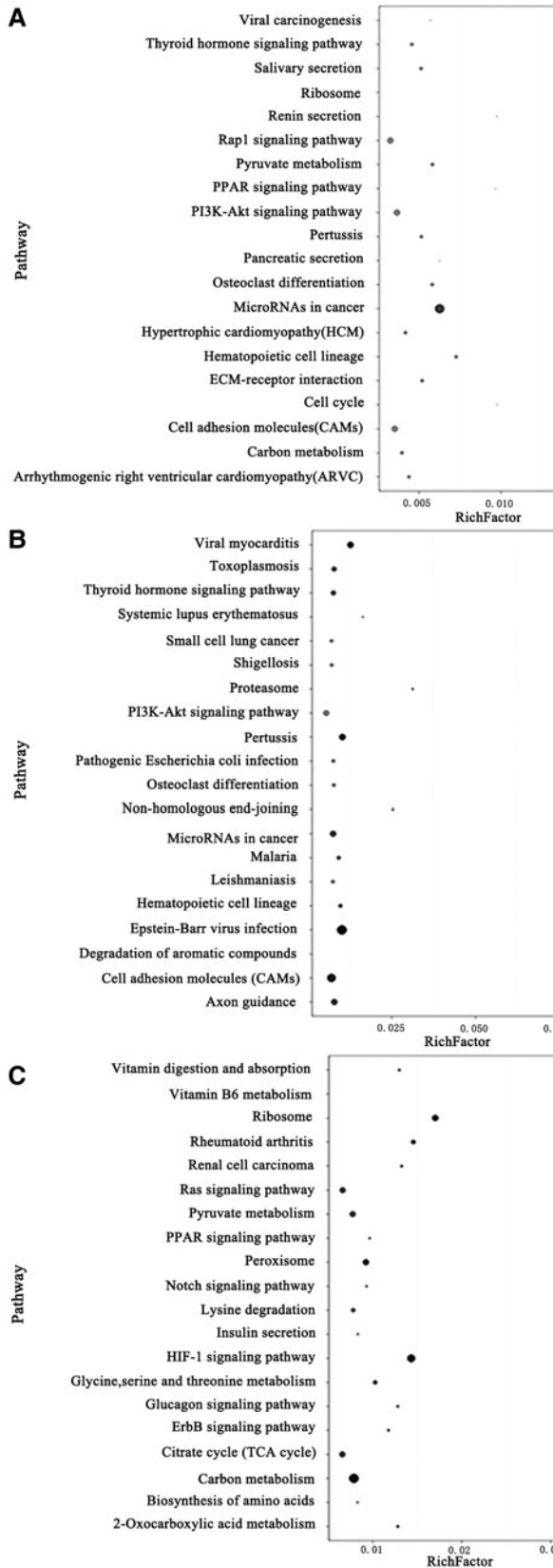
Fig. 3. Statistics for the pathway enrichment of DEGs in each pairwise comparison. 'RichFactor' is the ratio of the number of DEGs annotated to a pathway term relative to all the genes annotated for this pathway term. A higher 'RichFactor' indicates greater intensity. The Q-value is the corrected P-value ranging from 0–1, where a lower Q-value denotes greater intensity. Only the top 20 enriched pathway terms are shown in the figure (A. DO2 vs DO4, B. DO2 vs DO8, C. DO4 vs DO8).
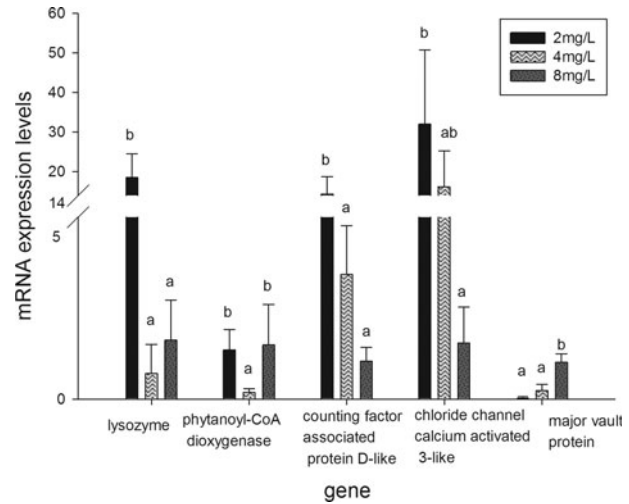

Fig. 4. Real-time qPCR analysis of five genes under DO2, DO4, and DO8. Different letters indicate significant differences between groups ($P < 0.05$). Values indicate the mean $\pm$ SD.

channel regulator 1 may mediate calcium-activated chloride conductance and it plays a critical role in calcium-activated chloride channels (Gruber et al., 1998). Calcium-activated chloride channel regulator 1-like was downregulated in *A. japonicus* under DO2 compared with DO4 and DO8, thereby indicating that the normal regulation of calcium-activated chloride channels was influenced under hypoxia.

Gamma-aminobutyric acid type B receptor subunit 1 is a component of a heterodimeric G-protein coupled receptor for gamma-aminobutyric acid. In the heterodimeric gamma-aminobutyric acid receptor, only the gamma-aminobutyric acid type B receptor subunit 1 may bind agonists. Ligand binding leads to a conformational change, which triggers signalling via G-proteins and activates downstream effectors. In this study, the downregulation of gamma-aminobutyric acid type B *receptor subunit 1-like* under a DO concentration of 2 mg l^{-1} might indicate that the signalling pathway related to the gamma-aminobutyric acid type B receptor subunit 1 in *A. japonicus* was restrained under hypoxia.

Genes associated with metabolism

When *A. japonicus* is exposed to stress due to hypoxia, various hypoxia survival mechanisms might be induced, where energy-consuming and ATP-generating pathways can be affected (Gracey et al., 2001).

Ribosomes are organelles that catalyse protein synthesis, and they comprise a small 40S subunit and a large 60S subunit. The 60S ribosomal protein L35 is a component of the 60S subunit, and the 40S ribosomal protein S24 is a component of the 40S subunit. Some ribosomal proteins are known to be expressed in both the intestine and respiratory tree in aestivated *A. japonicus* (Zhao et al., 2014), and when the animals discontinued using energy for feeding, weight loss occurred and anabolism decreased (Yuan et al., 2007). The differential expression of ribosomal proteins under different DO conditions is vitally important for protein synthesis inhibition, mRNA-rRNA processing and signal transduction (Kim & Jang, 2002; Warner & McIntosh, 2009). The downregulation of ribosomal proteins in *A. japonicus* under a DO

concentration of $2 \, \mathrm{mg \, l^{-1}}$ compared with $8 \, \mathrm{mg \, l^{-1}}$ might indicate the inhibition of normal protein synthesis, whereas the upregulation compared with a DO concentration of $4 \, \mathrm{mg \, l^{-1}}$ might be explained by the initiation of the synthesis of specific proteins that have functions associated with hypoxia.

In addition, genes associated with redox reactions, such as alcohol dehydrogenase [NADP+]-like, epidermal retinol dehydrogenase 2-like, and phytanoyl-CoA dioxygenase, peroxisomal-like also had different expression levels under various DO concentrations, and the corresponding metabolism function might have been affected.

Genes associated with immune defence

Apostichopus japonicus can only survive under a specific DO range, where a low DO concentration acts as a stimulus and certain biological processes will be induced to respond to or resist a changing environment, and thus immune defence processes may be affected and function in an disordered manner.

Lysozyme is a component of the innate immune system. Lysozyme is abundant in a number of secretions. It is also present in cytoplasmic granules in polymorphonuclear neutrophils and macrophages. Immunoglobulin G (IgG) complexes are associated with numerous functions, where they are responsible for the lytic potential of cytotoxic lymphocytes and monocytes, and they regulate the activation of B lymphocytes via different receptors when IgGFc is expressed on different cells (Ravetch & Kinet, 1991). The downregulation of *lysozyme* and *IgGFc-binding protein, partial* in *A. japonicus* under DO2 compared with DO4 and DO8 suggest that the basic immune system could be affected by hypoxia in *A. japonicus*.

Fibrinogen is the principal protein responsible for blood clotting in vertebrates and its major function is as the precursor to fibrin. Fibrin also plays a key role in the inflammatory response (Gilliam et al., 2011). The different expression levels of fibrinogen C domain-containing protein 1-B, partial, fibrinogen-like protein 1-like and fibrinogen-like protein A in *A. japonicus* under low DO conditions might indicate a disordered immune defence system.

Genes associated with hypoxia

When *A. japonicus* is stressed by hypoxia, some genes that are directly associated with hypoxia may be over-expressed. Angiopoietin-like 4 is induced under hypoxic conditions in various cell types and it is the target of peroxisome proliferator-activated receptors (Kim et al., 2011). The encoded protein is a serum hormone, which is directly involved in the regulation of lipid metabolism. The overexpression of angiopoietin-related protein 4-like in *A. japonicus* under DO2 compared with DO4 and DO8 may be an indicator of the reaction to hypoxia.

Genes that are related to redox reactions associated with hypoxia were also involved. Thioredoxins were upregulated in *A. japonicus* under DO2 and DO4 compared with DO8, and they play important roles in maintaining cellular homeostasis in all living organisms. They participate in many important biological processes, including the positive regulation of various redox reactions via the reversible oxidation of its active centre dithiol to a disulphide, as well as catalysing dithiol-disulphide exchange reactions (Lemaire, 2004; Park et al., 2012).

REFERENCES

Abdi H. (2007) The Bonferonni and Šidák corrections for multiple comparisons. *Encyclopedia of Measurement and Statistics* 3, 103–107.

Deutsch C., Brix H., Ito T., Frenzel H. and Thompson L. (2011) Climate-forced variability of ocean hypoxia. *Science* 333, 336–339.

Diaz R.J. (2001) Overview of hypoxia around the world. *Journal of Environmental Quality* 30, 275–281.

Diaz R.J. and Rosenberg R. (1995) Marine benthic hypoxia: a review of its ecological effects and the behavioural responses of benthic macrofauna. *Oceanography and Marine Biology: An Annual Review* 33, 245–303.

Dong Y., Dong S. and Meng X. (2008) Effects of thermal and osmotic stress on growth, osmoregulation and Hsp70 in sea cucumber (*Apostichopus japonicus* Selenka). *Aquaculture* 276, 179–186.

Du H., Bao Z., Hou R., Wang S., Su H., Yan J., Tian M., Li Y., Wei W., Lu W., Hu X., Wang S. and Hu J. (2012) Transcriptome sequencing and characterization for the sea cucumber *Apostichopus japonicus* (Selenka, 1867). *PLoS ONE* 7, e33311.

Eggermont J. (2004) Calcium-activated chloride channels. *Proceedings of the American Thoracic Society* 1, 22–27.

Gilliam B.E., Reed M.R., Chauhan A.K., Dehlendorf A.B. and Moore T.L. (2011) Evidence of fibrinogen as a target of citrullination in IgM rheumatoid factor-positive polyarticular juvenile idiopathic arthritis. *Pediatric Rheumatology* 9, 1–10.

Gracey A.Y., Troll J.V. and Somero G.N. (2001) Hypoxia-induced gene expression profiling in the euryoxic fish *Gillichthys mirabilis*. *Proceedings of the National Academy of Sciences USA* 98, 1993–1998.

Grantham B.A., Chan F., Nielsen K.J. and Fox D.S. (2004) Upwelling-driven nearshore hypoxia signals ecosystem and oceanographic changes in the northeast Pacific. *Nature* 429, 749–754.

Gruber A.D., Elble R.C., Ji H.-L., Schreur K.D., Fuller C.M. and Pauli B.U. (1998) Genomic cloning, molecular characterization, and functional analysis of human CLCA1, the first human member of the family of Ca 2^+-activated Cl$^-$ channel proteins. *Genomics* 54, 200–214.

Hemandezl V., Robles M. and Talon M. (2006) Blast2GO goes grid: developing a grid-enabled prototype for functional genomics analysis. In *Proceedings of the Challenges and Opportunities of Healthgrids: Proceedings of Healthgrid.*

Holm K., Hernroth B. and Thorndyke M. (2008) Coelomocyte numbers and expression of HSP70 in wounded sea stars during hypoxia. *Cell and Tissue Research* 334, 319–325.

Kashenko S. (2000) Acclimation of the sea cucumber *Apostichopus japonicus* to decreased salinity at the blastula and gastrula stages: its effect on the desalination resistance of larvae at subsequent stages of development. *Russian Journal of Marine Biology* 26, 422–426.

Kim D., Langmead B. and Salzberg S.L. (2015) HISAT: a fast spliced aligner with low memory requirements. *Nature Methods* 12, 357–360.

Kim S.-H., Park Y.-Y., Kim S.-W., Lee J.-S., Wang D. and DuBois R.N. (2011) ANGPTL4 induction by prostaglandin E2 under hypoxic conditions promotes colorectal cancer progression. *Cancer Research* 71, 7010–7020.

Kim Y.K. and Jang S.K. (2002) Continuous heat shock enhances translational initiation directed by internal ribosomal entry site. *Biochemical and Biophysical Research Communications* 297, 224–231.

Langmead B., Trapnell C., Pop M. and Salzberg S.L. (2009) Ultrafast and memory-efficient alignment of short DNA sequences to the human genome. *Genome Biology* 10, 1.

Lemaire S.D. (2004) The glutaredoxin family in oxygenic photosynthetic organisms. *Photosynthesis Research* 79, 305–318.

Li B. and Dewey C.N. (2011) RSEM: accurate transcript quantification from RNA-Seq data with or without a reference genome. *BMC Bioinformatics* 12, 1.

Li L. and Li Q. (2010) Effects of stocking density, temperature, and salinity on larval survival and growth of the red race of the sea cucumber *Apostichopus japonicus* (Selenka). *Aquaculture International* 18, 447–460.

Liao Y. (1980) The aspidochirote holothurians of China with erection of a new genus. In *Proceedings of the European Colloquium on Echinoderms*, pp. 115–120.

Meng X., Dong Y., Dong S., Yu S. and Zhou X. (2011) Mortality of the sea cucumber, *Apostichopus japonicus* Selenka, exposed to acute salinity decrease and related physiological responses: osmoregulation and heat shock protein expression. *Aquaculture* 316, 88–92.

Mortazavi A., Williams B.A., McCue K., Schaeffer L. and Wold B. (2008) Mapping and quantifying mammalian transcriptomes by RNA-Seq. *Nature Methods* 5, 621–628.

Nestlerode J.A. and Diaz R.J. (1998) Effects of periodic environmental hypoxia on predation of a tethered polychaete, *Glycera americana*: implications for trophic dynamics. *Marine Ecology Progress Series* 172, 185–195.

Nilsson H.C. and Sköld M. (1996) Arm regeneration and spawning in the brittle star *Amphiura filiformis* (O.F. Müller) during hypoxia. *Journal of Experimental Marine Biology and Ecology* 199, 193–206.

Oweson C., Li C., Söderhäll I. and Hernroth B. (2010) Effects of manganese and hypoxia on coelomocyte renewal in the echinoderm, *Asterias rubens* (L.). *Aquatic Toxicology* 100, 84–90.

Pan Y., Zhang L., Lin C., Sun J., Kan R. and Yang H. (2015) Influence of flow velocity on motor behavior of sea cucumber *Apostichopus japonicus*. *Physiology & Behavior* 144, 52–59.

Park C.-I., Jung J.-H., Shim W.-J., Kim J.-W., Kim E.-G., Jeong J.-M. and Kim D.-H. (2012) Molecular characterization, expression, and functional analysis of two thioredoxins in the black rockfish (*Sebastes schlegelii*). *Fish & Shellfish Immunology* 32, 808–815.

Ravetch J.V. and Kinet J.-P. (1991) Fc receptors. *Annual Review of Immunology* 9, 457–492.

Ren J.S., Stenton-Dozey J. and Zhang J. (2017) Parameterisation and application of dynamic energy budget model to sea cucumber *Apostichopus japonicus*. *Aquaculture Environment Interactions* 9, 1–8.

Shao Y., Li C., Ou C., Zhang P., Lu Y., Su X., Li Y. and Li T. (2013) Divergent metabolic responses of *Apostichopus japonicus* suffered from skin ulceration syndrome and pathogen challenge. *Journal of Agricultural and Food Chemistry* 61, 10766–10771.

Shick J.M. (1976) Physiological and behavioral responses to hypoxia and hydrogen sulfide in the infaunal asteroid *Ctenodiscus crispatus*. *Marine Biology* 37, 279–289.

Siikavuopio S.I., Dale T., Mortensen A. and Foss A. (2007) Effects of hypoxia on feed intake and gonad growth in the green sea urchin, *Strongylocentrotus droebachiensis*. *Aquaculture* 266, 112–116.

Sloan N.A. (1984) Echinoderm fisheries of the world: a review. In Keegan B.F. and O'Connor B.D.S. (eds) *Echinodermata*. Rotterdam: A.A. Balkema Publishers, pp 109–124.

Sui J., Dong S., Tian X., Wang F. and Dong Y. (2010) The effect of light color on re spiration and excretion of sea cucumber, *Apostichopus japonicus*. *Periodical of Ocean University of China* 40, 61–64. [In Chinese, with English abstract]

Sun J., Zhang L., Pan Y., Lin C., Wang F., Kan R. and Yang H. (2015) Feeding behavior and digestive physiology in sea cucumber *Apostichopus japonicus*. *Physiology & Behavior* 139, 336–343.

Sun L., Chen M., Yang H., Wang T., Liu B., Shu C. and Gardiner D.M. (2011) Large scale gene expression profiling during intestine and body wall regeneration in the sea cucumber *Apostichopus japonicus*. *Comparative Biochemistry and Physiology Part D: Genomics and Proteomics* 6, 195–205.

Sun L., Yang H., Chen M., Ma D. and Lin C. (2013) RNA-Seq reveals dynamic changes of gene expression in key stages of intestine regeneration in the sea cucumber *Apostichopus japonicus*. *PLoS ONE* 8, e69441.

Tarazona S., García-Alcalde F., Dopazo J., Ferrer A. and Conesa A. (2011) Differential expression in RNA-seq: a matter of depth. *Genome Research* 21, 2213–2223.

Theede H., Ponat A., Hiroki K. and Schlieper C. (1969) Studies on the resistance of marine bottom invertebrates to oxygen-deficiency and hydrogen sulphide. *Marine Biology* 2, 325–337.

Vaquer-Sunyer R. and Duarte C.M. (2008) Thresholds of hypoxia for marine biodiversity. *Proceedings of the National Academy of Sciences USA* 105, 15452–15457.

Wang F., Yang H., Gao F. and Liu G. (2008) Effects of acute temperature or salinity stress on the immune response in sea cucumber, *Apostichopus japonicus*. *Comparative Biochemistry and Physiology Part A: Molecular & Integrative Physiology* 151, 491–498.

Wang F., Yang H., Wang X., Xing K. and Gao F. (2011) Antioxidant enzymes in sea cucumber *Apostichopus japonicus* (Selenka) during aestivation. *Journal of the Marine Biological Association of the United Kingdom* 91, 209–214.

Warner J.R. and McIntosh K.B. (2009) How common are extraribosomal functions of ribosomal proteins? *Molecular Cell* 34, 3–11.

Yuan X., Yang H., Wang L., Zhou Y. and Gabr H.R. (2010) Effects of salinity on energy budget in pond-cultured sea cucumber *Apostichopus japonicus* (Selenka) (Echinodermata: Holothuroidea). *Aquaculture* 306, 348–351.

Yuan X., Yang H., Wang L., Zhou Y., Zhang T. and Liu Y. (2007) Effects of aestivation on the energy budget of sea cucumber *Apostichopus*

japonicus (Selenka) (Echinodermata: Holothuroidea). *Acta Ecologica Sinica* 27, 3155–3161.

Zhang L., Pan Y. and Song H. (2015*a*) Environmental drivers of behavior. In Yang H., Hamel J.-F. and Mercier A. (eds) *The sea cucumber* Apostichopus japonicus: *history, biology and aquaculture.* Volume 39. Boston, MA: Academic Press, pp. 133–152.

Zhang L., Song X., Hamel J.-F. and Mercier A. (2015*b*) Aquaculture, stock enhancement, and restocking. In Yang H., Hamel J.-F. and Mercier A. (eds) *The sea cucumber* Apostichopus japonicus: *history, biology and aquaculture.* Volume 39. Boston, MA: Academic Press, pp. 289–322.

Zhang P., Li C., Zhang P., Jin C., Pan D. and Bao Y. (2014) iTRAQ-based proteomics reveals novel members involved in pathogen challenge in sea cucumber Apostichopus japonicus. *PLoS ONE* 9, e100492.

Zhang P., Li C., Zhu L., Su X., Li Y., Jin C. and Li T. (2013) De novo assembly of the sea cucumber *Apostichopus japonicus* hemocytes transcriptome to identify miRNA targets associated with skin ulceration syndrome. *PLoS ONE* 8, e73506.

Zhao Y., Yang H., Storey K.B. and Chen M. (2014) Differential gene expression in the respiratory tree of the sea cucumber *Apostichopus japonicus* during aestivation. *Marine Genomics* 18, 173–183.

and

Zhou Z.C., Dong Y., Sun H.J., Yang A.F., Chen Z., Gao S., Jiang J.W., Guan X.Y., Jiang B. and Wang B. (2014) Transcriptome sequencing of sea cucumber (*Apostichopus japonicus*) and the identification of gene-associated markers. *Molecular Ecology Resources* 14, 127–138.

Correspondence should be addressed to:
H. Yang
CAS Key Laboratory of Marine Ecology and Environmental Sciences, Institute of Oceanology, Chinese Academy of Sciences, 7 Nanhai Road, Qingdao 266071, China
email: hshyang@qdio.ac.cn